**Homeobox B9 mediates resistance to anti-VEGF therapy in colorectal cancer patients**

Carbone, Carmine; Piro, Geny; Simionato, Francesca; Ligorio, Francesca; Cremolini, Chiara; Loupakis, Fotios; Alì, Greta; Rossini, Daniele; Merz, Valeria; Santoro, Raffaela; Zecchetto, Camilla; Zanotto, Marco; Di Nicolantonio, Federica; Bardelli, Alberto; Fontanini, Gabriella; Tortora, Giampaolo; Melisi, Davide. Homeobox B9 mediates resistance to anti-VEGF therapy in colorectal cancer patients. CLINICAL CANCER RESEARCH. None pp: 1-12.
DOI: 10.1158/1078-0432.CCR-16-3153

**Homeobox B9 mediates resistance to anti-VEGF therapy in colorectal cancer patients**

Carmine Carbone[1,†], Geny Piro[1,2,†], Francesca Simionato[3], Francesca Ligorio[1], Chiara Cremolini[4], Fotios Loupakis[5], Greta Alì[6], Daniele Rossini[4], Valeria Merz[3], Raffaela Santoro[1], Camilla Zecchetto[3], Marco Zanotto[1], Federica Di Nicolantonio[7,8], Alberto Bardelli[8], Gabriella Fontanini[6], Giampaolo Tortora[2,3], and Davide Melisi[1,3,].

[1]Digestive Molecular Clinical Oncology Research Unit, Department of Medicine, Università degli studi di Verona, Verona, Italy; [2]Laboratory of Oncology and Molecular Therapy, Department of Medicine, Università degli studi di Verona, Verona, Italy; [3]Medical Oncology Unit, Azienda Ospedaliera Universitaria Integrata, Verona, Italy; [4]Polo Oncologico, Azienda Ospedaliero-Universitaria Pisana, Istituto Toscano Tumori, Pisa, Italy University of Pisa, Pisa, Italy; [5]Unit of Oncology 1, Istituto Oncologico Veneto IRCCS, Padova, Italy; [6]Division of Pathology, Department of Surgical, Medical, Molecular Pathology, and Critical Area, University of Pisa, Pisa, Italy; [7]Department of Oncology, University of Torino, Candiolo, Italy; [8]Candiolo Cancer Institute-FPO, IRCCS, Candiolo, Italy.

[†]These authors contributed equally to this work.

**Running Title:** HOXB9 in anti-VEGF resistance

**Keywords:** Gastrointestinal cancers: colorectal, Anti-VEGF, angiogenesis.

**Grant Support:** This work was supported by the Investigator Grant n°19111 to DM and n°18599 to GT through the Associazione Italiana per la Ricerca sul Cancro (AIRC), and by the Basic Research Project 2015 through the University of Verona to DM.

**Disclosure of Potential Conflicts of Interest:** No potential conflicts of interest to disclose.

**Correspondence to**: Davide Melisi, MD, PhD, Digestive Molecular Clinical Oncology unit, Section of Medical Oncology, Department of Medicine, University of Verona, AOUI Verona - Policlinico "G.B. Rossi", Piazzale L.A. Scuro,10, 37134 - Verona - Italy (email: davide.melisi@univr.it).

## TRANSLATIONAL RELEVANCE

The identification of predictive biomarkers for antiangiogenic therapies poses one of the greatest challenges in digestive cancer research. We demonstrated HOXB9 as crucial transcription factor to sustain tumor resistance to bevacizumab, and that silencing its expression could be a promising approach to modulate this resistance. Our results candidate HOXB9 as novel biomarker for selecting patients with colorectal cancer for antiangiogenic therapy.

## ABSTRACT

**Purpose:** The identification of predictive biomarkers for antiangiogenic therapies remains an unmeet need. We hypothesized that the transcription factor Homeobox B9 (HOXB9) could be responsible for the tumor resistance to the anti-VEGF agent bevacizumab.

**Experimental Design:** HOXB9 expression and activation were measured in eight models of colorectal and pancreatic cancer with different resistance to bevacizumab. Serum levels of Angiopoietin-like Protein (Angptl)2, CXC receptor ligand (CXCL)1, interleukin(IL)8, and Transforming Growth Factor (TGF)β1 in tumor-bearing mice were measured by multiplex xMAP technology. HOXB9 expression was measured by immunohistochemical analysis in 81 pretreatment specimens from metastatic colorectal cancer patients. Differences in progression-free survival (PFS) were determined using a log-rank test.

**Results:** HOXB9-positive tumors were resistant to bevacizumab, whereas mice bearing HOXB9-negative tumors were cured by this agent. Silencing HOXB9 in bevacizumab-resistant models significantly ($P$<0.05) reduced Angptl2, CXCL1, IL8, and TGFβ1 levels, reverted their mesenchymal phenotype, reduced CD11b+ cells infiltration, and restored, in turn, sensitivity to bevacizumab. HOXB9 had no prognostic value in patients treated with a first-line chemotherapeutic regimen non-containing bevacizumab. However, patients affected by an HOXB9-negative tumor had a significantly longer PFS compared with those with an HOXB9-positive tumor if treated with a first-line regimen containing bevacizumab (18.0 months vs 10.4 months; HR=2.037; 95% CI=1.006-4.125; $P$=0.048).

**Conclusions:** These findings integrate the complexity of numerous mechanisms of anti-VEGF resistance into the single transcription factor HOXB9. Silencing HOXB9 could be a promising approach to modulate this resistance. Our results candidate HOXB9 as predictive biomarker for selecting colorectal cancer patients for antiangiogenic therapy.

## INTRODUCTION

Angiogenesis is a hallmark of cancer and its inhibition is commonly part of the therapeutic strategies for several tumor types (1,2). Bevacizumab, a humanized monoclonal antibody targeting Vascular Endothelial Growth Factor (VEGF) has been the most extensively studied antiangiogenic agent in digestive tumors, and, in particular, the first to be approved for the treatment of metastatic colorectal cancer (3). However, the preexistence or the rapid development of molecular mechanisms of resistance to the inhibition of VEGF limit the efficacy of bevacizumab in the treatment of colorectal cancer patients (4), and leaded to its failing in other digestive tumors, including pancreatic cancer (5,6).

Although predictive biomarkers would be urgently needed in order to maximize clinical benefit, avoid unnecessary drug toxicity, and improve costs of cancer care, no biomarker exists for antiangiogenic drugs to date, and these agents are usually given to unselected patients for the approved indications (7,8). In the last decade, most of the efforts in defining valid biomarkers of response to antiangiogenic drugs in clinical trials seemed neglectful of the results of those preclinical studies revealing the actual molecular mechanisms responsible for tumor resistance to these agents. Whereas a number of clinical studies simply explored plasma levels or genetic polymorphisms of components of the VEGF signaling pathway as biomarker for bevacizumab outcome (9), numerous preclinical studies contributed to depict a much more intricate scenario of alternative proangiogenic and proinflammatory cytokines available to the tumor and its stromal components to resist the activity of antiangiogenic drugs [reviewed in (10,11)]. The complexity of these mechanisms could explain the difficulty to identify a binary biomarker, easy to be measured and interpreted, and to be embedded into large randomized clinical trials (12).

We recently contributed to this field by demonstrating the overexpression of a signature of proinflammatory and proangiogenic factors – including Angiopoietin-like Protein (Angptl)2, CXC receptors (CXCR)1/2 ligands such as CXCL1 and interleukin(IL)8, IL1 $\alpha$ and $\beta$, and Transforming

Growth Factor (TGF)β1 – in bevacizumab-resistant preclinical models if compared to their sensitive counterparts. These factors indirectly sustained angiogenesis through the recruitment of $CD11b^+$ myeloid cells, and increased the aggressiveness of bevacizumab-resistant tumors by inducing epithelial-to-mesenchymal transition (EMT) (13). The combined inhibition of IL1, CXCR1/2, and TGFβ signaling pathways modulated in vivo bevacizumab-resistance by reversing EMT and inhibiting $CD11b^+$ cells' tumor infiltration (14).

Homeobox B9 (HOXB9) belongs to the highly conserved homeobox transcription factor gene family, which is critical for embryonic development. In cancer, Hox genes expression directly drives neoplastic transformation and tumor progression through escape from apoptosis, alterations to receptor signaling, EMT, and tumor cell invasion (15). In particular, HOXB9 enhanced the competence of lung adenocarcinoma cells to form bone and the brain metastases (16). In breast cancer, the overexpression of HOXB9 induced cell motility and an EMT phenotype (17), and increased the expression of TGFβ, IL8 and ANGPTL2 (18). In a large cohort of breast cancer patients, HOXB9 was a highly significant prognostic factor. In particular, HOXB9-positive tumors showed a significant increase in the number of vasculature compared with HOXB9-negative tumors (19).

In this present study, we hypothesized that HOXB9 could be responsible for the resistance of digestive tumors to the antiangiogenic drug bevacizumab by coordinating the transcription of the proinflammatory and proangiogenic factors Angptl2, CXCL1, IL8, and TGFβ1. Thus, measuring the expression of HOXB9 might serve as potential biomarker to select patients with colorectal cancer more likely to benefit from antiangiogenic drugs.

## MATERIALS AND METHODS

### Cell Lines and generation of HOXB9 knockdown cell lines.

All cell lines were maintained in their original culturing conditions according with supplier guidelines. Cells were ordinarily supplemented with fetal bovine serum, 2 mM L-glutamine, antibiotics (100 U ml−1 penicillin and 100 mg ml−1 streptomycin) and grown in a 37 °C and 5% CO2 air incubator. Cells were daily checked by morphology and routinely tested to be Mycoplasma free by PCR assay. $RFP^+$ HOXB9-$shRNA^+$ cell lines were obtained by lentiviral infection as described in supplementary materials.

### Cell Proliferation Assay

On day 0, $1.0x10^3$ cells/well were seeded in 96-well plates. At the indicated hours, sulforhodamine B (SRB) (Sigma, St. Louis, Missouri, USA) assay was used to obtain relative estimates of viable cell number. Briefly, trichloroacetic acid fixed cells were stained for 30 minutes with 0.4% SRB dissolved in 1% acetic acid. SRB was removed and cultures were quickly rinsed four times with 1% acetic acid to remove unbound dye. After being rinsed, the cultures were air dried until no standing moisture was visible. Bound dye was resuspended in Tris 10mM pH 10,5 and read with iMark Microplate Absorbance Reader spectrophotometer (Bio-Rad Lab., Inc., Hercules, California, USA) at 540 nm.

### Protein extraction and western blotting

Cell lines were washed twice with cold phosphate-buffered saline and lysed at 4°C into RIPA buffer (50 mM Tris–HCl [pH 8], 150 mM NaCl, 1% Nonidet P-40, 0.5% sodium deoxycholate, and 0.1% sodium dodecyl sulfate) plus protease inhibitor mix (Sigma-Aldrich). Lysates were clarified by centrifugation and protein concentrations. Each lysate was separated by SDS-PAGE and probed with antibodies against E-Cadherin, HOXB9 (Abcam, Cambridge, UK), Histone H3 (Cell Signaling Technology, Boston, MA), vimentin (Dako, Denmark), and γ-tubulin, (Santa Cruz Biotechnology, Santa

Cruz, CA). Immunoreactive proteins were detected using an enhanced-chemiluminescence reagent (ECL, Millipore, Billerica, MA) according to the manufacturer's instructions. Images were captured by LAS4000 Digital Image Scanning System (GE Healthcare, Little Chalfont, UK).

**Electrophoretic mobility shift assay (EMSA) and DNA affinity precipitation assay (DAPA)**

Nuclear extracts of pancreatic and colorectal cancer cell lines were prepared according to the method of Andrews and Faller (20). For EMSA assay, the wild-type double-stranded oligonucleotides containing the HOXB9 and control sequence site was obtained from Santa Cruz Biotechnology, Inc. and labeled with 32P to be used as probes. Instead, HOXB9-specific biotinylated oligodeoxynucleotides and control sequences were used for DAPA assay. The reactions were analyzed on 4% polyacrylamide gels containing 0.25X TBE buffer.

**Immunofluorescence**

Pancreatic cancer cell lines COLO357FG and FGBR, and colorectal cancer cell lines MDST8 and GP5D, were cultured for 24 hours on cover slips in a 24 multi-well, fixed with 2.5% formalin and permeabilized with 0.1% Triton for 10 minutes at 4°C. The cells were then incubated with the primary antibody specific for HOXB9 (Abcam, Cambridge, UK) for 1 hour at room temperature and with fluorophore (FITC)–conjugated as secondary antibody. Nuclei were stained with Hoechst 33342 (blue). Cover slips were mounted with pro-long antifade mountant (Invitrogen, Carlsbad, CA, USA). The images were obtained with a confocal microscopy (LMS510, Zeiss, Oberkochen, Germany).

**Wound Healing Migration assay**

Cell lines were seeded to 90% of confluence in 100 mm cell culture dishes. After 24 hours cells a straight scratch was made using a pipette tip to simulate a wound. The cells were washed gently with cold PBS 1X and rinsed with fresh medium. Photographs at five different points at least were taken immediately and after 24 and 36 hours of culture.

**Gene Expression Microarray and Pathway Analysis**

Differences in gene expression between cell lines were examined using Illumina Human 44k gene chips (Illumina, Milan, Italy). Briefly, synthesis of cDNA and biotinylated cRNA was performed using the IlluminaTotalPrep RNA Amplification Kit (Ambion), according to the manufacturer's protocol using 500ng of total RNA. Hybridization of cRNAs (750 ng) was carried out using Illumina Human 48k gene chips (Human HT-12 V4 BeadChip). Array washing was performed using Illumina High Temp Wash Buffer for 10' at 55°C, followed by staining using streptavidin-Cy3 dyes (Amersham Biosciences). Probe intensity data were obtained using the Illumina Genome Studio software (Genome Studio V2011.1). Raw data were Loess normalized with the Lumi R package and further processed with Excel software. Each microarray experiment was repeated twice. Differentially expressed transcripts were tested for network and functional interrelatedness using the IPA software program (Ingenuity Systems, Redwood, CA). Gene expression microarray data have been deposited in the GEO database with accession number (GSE59857).

**RNA Isolation and Quantitative RT-PCR Assay**

Total RNA was obtained from cells using Trizol reagent (Invitrogen, Carlsbad, CA, USA) according to manufacturer's instructions. Total RNA was quantified by absorbance at 260 nm. Reverse transcription was performed using the High Capacity Reverse Transcription Kit (Qiagen, Venlo, Netherlands). The cDNA obtained was evaluated for Real-Time PCR with ABI Prism 7900 HT Sequence Detection System (Applied Biosystems, Foster City, CA, USA) using specific primer and SYBR Green. QuantiTect Primer Assays (Qiagen, Venlo, Netherlands) were used to quantify cDNA levels of CDH1, VIM, ANGPTL2, CXCL1, IL1A, IL1B, CXCL8, VEGFa, TGFβ2 and β-Actin. Gene expression was calculated using $2^{-\Delta\Delta}$CT method and normalized to β-actin expression.

**Xenograft Model in Nude Mice**

The orthotopic injection of luc+/GFP+ pancreatic cancer cells and the subcutaneous heterotopic implantation of colorectal and pancreatic cancer cells was performed as described previously in (21,22). Tumor bearing mice were randomly assigned (n=5 per group) to receive 100 μg of bevacizumab i.p. twice a week or saline as a control. In mice bearing heterotopic xenografts, the tumor size was measured with a caliper. Mice were euthanized using carbon dioxide inhalation when evidence of advanced bulky disease developed or at cut-off volume of 2 $cm^3$, which was considered the day of death for the purpose of survival evaluation. Animal study was approved by the local ethics committee. Additional details of methods are provided in Supplementary Methods section.

**BioPlex and ELISA for cytokines detection in murine plasma**

Multiplex biometric ELISA based immunoassay was performed according to the manufacturer's instructions (Bioplex, Bio-Rad Lab., Inc., Hercules, CA, USA). Soluble molecules were measured in murine plasma using a commercially available kit which provides a series of combined reagents for the simultaneous measurement of human cytokines in serum, plasma, or tissue culture supernatant. Each experiment was performed in duplicate. Serum levels of all proteins were determined using a Bio-Plex array reader (Bio-Rad Lab., Hercules, CA, USA) that quantitates multiplex immunoassays in a 96-well format with very small fluid volumes. The analytes concentration was calculated using a standard curve, with software provided by the manufacturer (Bio-Plex Manager Software). ANGPTL2 quantification in murine plasma was performed by hANGPTL2 ELISA (Cusabio Biotech Co.) following the manufacterer's instructions.

**Patients**

81 patients with metastatic colorectal cancer were included in the retrospective study. 58 patients underwent first-line bevacizumab-based therapy and 23 did not receive bevacizumab. HOXB9 protein

expression in patient tissue samples was compared by immunohistochemical analyses. Informed consent was obtained from all patients. REMARK guidelines compliance is reported in supplementary table S2.

**Statistical Analysis**

Progression-free survival (PFS) was calculated as the period from the first day of treatment to the date of tumor progression. PFS curves were drawn by Kaplan-Meier estimates and compared by log rank test. Univariate and multivariate analyses of PFS with stepwise variable selection were conducted by Cox's proportional hazard regression models. Multivariate analysis was conducted using the variables that were significant in univariate analysis ($P \leq 0.05$). The relationship between HOXB9 expression and clinic-pathological characteristics was examined using the $\chi 2$ method for linear trend. Additional details of methods are provided in Supplementary Methods section.

## RESULTS

### Silencing HOXB9 Modulates Anti-VEGF Resistance In Pancreatic Cancer Models

To test the hypothesis that HOXB9 could be responsible for the anti-VEGF resistance in digestive tumors, we initially studied its role in the bevacizumab-resistant FGBR pancreatic cancer model established in (13). We verified that COLO357FG tumors were sensitive to bevacizumab, whereas mice bearing FGBR tumors exhibited resistance showing survival rates similar to untreated control mice (Figure 1A). We also confirmed that the expression of the epithelial marker E-cadherin was suppressed, and that of the mesenchymal marker Vimentin was strongly upregulated in FGBR if compared with COLO357FG cells (Supplementary Figure 1A). Although they had similar proliferation rates (Supplementary Figure 1B), the FGBR cells had a significantly higher migration rate than did COLO357FG cells (Supplementary Figure 1C).

We demonstrated that FGBR cells had significantly higher nuclear expression levels of HOXB9 than did COLO357FG cells (Figure 1, B and C). Consistently, we measured an increased HOXB9 DNA-binging activity in FGBR compared with COLO357FG cells (Figure 1D, and Supplementary Figure 1A). When orthotopically injected in nude mice, FGBR tumors exhibited a significantly stronger expression of HOXB9 than did COLO357FG tumors (Figure 1E). Importantly, we measured significantly higher plasma levels of human Angptl2, CXCL1, IL8, and TGFβ1 in mice bearing FGBR tumors then in those bearing COLO357FG tumors (Figure 1F).

To demonstrate the role of HOXB9 in sustaining resistance to bevacizumab, we knocked-down the expression of HOXB9 in FGBR cells by transducing them with lentiviruses expressing HOXB9-specific shRNAs or a scramble sequence as control (Figure 1G, and Supplementary Figure 2A). Consistently, HOXB9 knockdown FGBR cells had a reduced HOXB9 DNA-binding activity compared with control and scramble cells (Figure 1H).

We measured a significantly reduced expression of ANGPTL2, CXCL1, IL8, and TGFβ1 genes in HOXB9 knockdown FGBR cells (Supplementary Figure 2B). As a consequence, silencing HOXB9

modulated EMT in bevacizumab-resistant FGBR cells by inducing a re-expression of E-cadherin at levels comparable with that of the bevacizumab-sensitive COLO357FG cells, and reducing the expression of Vimentin (Figure 1I). Although they had similar proliferation rates (Supplementary Figure 2C), HOXB9 knockdown FGBR cells exhibited a significantly reduced migration rate compared with control cells (Figure 1J).

Moreover we inhibited HOXB9 transcriptional activity by treating FGBR cells with an HOXB9 decoy oligodeoxynuclotide (ODN) or a mutant ODN as control. Although no significant difference was observed in the proliferation rate upon treatment with either the HOXB9 decoy ODN or mutant ODN, HOXB9 decoy ODN induced a statistically significant reduction of migration rate respect to mutant ODN or untreated cells (Supplementary Figure 3).

To confirm the role of HOXB9 in resistance to bevacizumab in vivo, twenty mice were orthotopically injected with HOXB9 knockdown or scramble FGBR cells and randomly assigned to be treated with bevacizumab or its ip vehicle as control (n=5). Initially, we measured significantly lower plasma levels of human Angptl2, CXCL1, IL8, and TGFβ1 in mice bearing HOXB9 knockdown FGBR tumors then in those bearing scramble FGBR tumors as control at baseline (Figure 2A). HOXB9 knockdown FGBR tumors had a lower expression level of HOXB9, higher expression of E-cadherin, and reduced expression of Vimentin than did scramble FGBR tumors (Figure 2B). At necropsy, the gross pathology of scramble FGBR control tumors revealed a highly vascularized structure, whereas HOXB9 knockdown FGBR tumors appeared clearly hypovascular (Figure 2C). Consistently, HOXB9 knockdown FGBR tumors demonstrated significantly lower infiltration by CD11b+ proangiogenic myeloid cells than did than did scramble FGBR tumors (Supplementary Figure 4).

Most importantly, only mice bearing HOXB9 knockdown FGBR tumors treated with bevacizumab experienced a statistically significant reduction in tumor growth, and demonstrated a statistically significantly prolonged median survival duration ($p<0.001$) if compared with vehicle-treated controls. Mice bearing scramble FGBR tumors treated with bevacizumab had tumor growth (Figure 2D) and survival rates comparable with those in vehicle-treated control mice (Figure 2E).

**HOXB9 Sustains Resistance To Anti-VEGF Therapy In Colorectal Cancer Models**

We set to extend our observations to colorectal cancer, a tumor type in which bevacizumab is widely applied in the clinic. To this end, we selected three HOXB9-positive – LOVO, MDST8, and LIM2099 – and three HOXB9-negative –CCK81, GP5D, and SNUC4– colorectal cancer cell lines (Figure 3A and B; Supplementary Figure 5, A and B) among a large collection of 151 colorectal cancer cell lines (23).

We initially measured a significantly higher expression of a number of proinflammatory and proangiogenic factors including ANGPTL2, CXCL1, IL1A, IL1B, IL8, and TGFβ1 in HOXB9-positive LOVO, MDST8, and LIM2099 cell lines than in HOXB9-negative CCK81, GP5D, and SNUC4 colorectal cancer cell lines (Figure 3C). Thus, HOXB9-positive cell lines demonstrated a more pronounced mesenchymal phenotype if compared with HOXB9-negative cell lines, with low expression levels of E-cadherin, high expression levels of Vimentin (Figure 3D), and a significantly higher migration rate (Supplementary Figure 5C).

To confirm the role of HOXB9 in resistance to bevacizumab of colorectal cancer models in vivo, forty mice were injected with HOXB9-positive MDST8 and LIM2099 or HOXB9-negative GP5D and CCK81 colorectal cancer cell lines and randomly assigned to be treated with i.p. bevacizumab or its vehicle as control (n=5). Interestingly, we measured lower plasma levels of human Angptl2, CXCL1, IL8, and TGFβ1 in mice bearing MDST8 or LIM2099 tumors than in those bearing GP5D or CCK81 tumors at baseline, with the exception of the high plasma levels of human Angptl2 in CCK81 tumor-bearing mice (Figure 3E). MDST8 and LIM2099 tumors had a higher expression level of HOXB9, lower expression of E-cadherin, and increased expression of Vimentin than did GP5D or CCK81 tumors (Figure 3F). Moreover, tumors with higher expression of HOXB9 had a greater infiltration by CD11b+ proangiogenic myeloid cells than did than HOXB9 negative tumors (Supplementary Figure 6). Most importantly, mice bearing HOXB9-positive LOVO or MDST8 were completely resistant to bevacizumab, whereas mice bearing HOXB9-negative GP5D and CCK81 colorectal cancer tumors were cured by the treatment with this anti-VEGF agent (Figure 3G).

To further demonstrate the role of HOXB9 in sustaining resistance to bevacizumab in colorectal cancer, we knocked-down HOXB9 expression in HOXB9-positive MDST8 cells by transducing them with lentiviruses expressing HOXB9-specific shRNAs or a scramble sequence as control (Figure 4A, and Supplementary Figure 7A). Consistently, HOXB9 knockdown MDST8 cells had a reduced HOXB9 DNA-binding activity compared with control and scramble cells (Supplementary Figure 7B). As consequence, we measured a significantly reduced expression of ANGPTL2, CXCL1, IL8, and TGFβ1 in HOXB9 knockdown MDST8 cells if compared with control cells (Supplementary Figure 7C). Although we could only measure a minimal reduction in the expression of the mesenchymal marker Vimentin (Supplementary Figure 7, D and E), HOXB9 knockdown MDST8 cells exhibited a significantly reduced migration rate compared with control cells (Figure 4B). Moreover, also HOXB9 transcriptional activity inhibition by decoy ODN induced a statistically significant reduction of migration rate respect to mutant ODN or untreated cells (Supplementary Figure 8).

To confirm the role of HOXB9 in resistance to bevacizumab in colorectal cancer models in vivo, twenty mice were orthotopically injected with HOXB9 knockdown or scramble MDST8 cells and randomly assigned to be treated with bevacizumab or its ip vehicle as control (n=5). We measured significantly lower plasma levels of human Angptl2, CXCL1, and IL8 in mice bearing HOXB9 knockdown MDST8 tumors then in those bearing scramble MDST8 tumors as control at baseline (Figure 4C). HOXB9 knockdown MDST8 tumors demonstrated a complete suppression of the expression of HOXB9, higher expression of E-cadherin, and reduced expression of Vimentin than did scramble MDST8 tumors (Figure 4D). At necropsy, the gross pathology of HOXB9 knockdown MDST8 tumors appeared clearly hypovascular if compared with scramble MDST8 control tumors (Figure 4E). Consistently, HOXB9 knockdown MDST8 tumors demonstrated significantly lower infiltration by CD11b+ proangiogenic myeloid cells than did scramble MDST8 tumors (Supplementary Figure 9).

Most importantly, mice bearing scramble MDST8 tumors treated with bevacizumab had tumor growth and survival rates comparable with those in vehicle-treated control mice. Conversely, mice bearing HOXB9 knockdown MDST8 tumors treated with bevacizumab experienced a statistically

significant reduction in tumor growth (Figure 4F), and demonstrated a statistically significantly prolongation of their median survival duration if compared with vehicle-treated controls (scramble MDST8 vs. HOXB9 knockdown MDST8, median survival=60 vs 79.5 days, *P*=0.0025) (Figure 4G).

**HOXB9 expression is an independent predictive factor for progression free survival in metastatic colorectal cancer patients treated with bevacizumab**

In order to confirm the clinical relevance of HOXB9 as predictive biomarker for bevacizumab treatment in colorectal cancer, we conducted an exploratory retrospective analysis of 81 metastatic patients who received first-line standard chemotherapeutic regimens in combination (n=58) or not (n=23) with bevacizumab. Patients' clinical characteristics and compliance with REMARK guidelines are reported in supplementary table S1 and S2, respectively.

Specimens obtained from patients at treatment baseline were evaluated for HOXB9 expression levels by immunohistochemical analysis, and tumor samples entirely or partially stained were classified as HOXB9-positive. Of the 81 specimens, 19 (23.46%) scored negatively and 62 (76.54%) scored positively.

In the cohort of patients treated with a first-line chemotherapeutic regimen non-containing bevacizumab, HOXB9 expression could not distinguish patients with different progression free survival (PFS) duration (HOXB9-positive median PFS=10.1 months vs HOXB9-negative median PFS=7.9 months; HR= 2.0004; 95% CI=0.576-6.967; *P*=0.27) (Figure 5A). Conversely, in the cohort of patients treated with a bevacizumab-containing first-line chemotherapeutic regimen we demonstrated that patients with HOXB9-negative tumors had a significantly longer PFS duration than did those with HOXB9-positive tumors (HOXB9-positive median PFS=10.4 months vs HOXB9-negative median PFS=18.0 months; HR=2.037; 95% CI=1.006-4.125; *P*=0.048) (Figure 5B). Univariate analysis revealed that primary tumor size, ECOG performance status, KRAS/NRAS/BRAF mutational status, and HOXB9 expression correlate with PFS in patients treated with a bevacizumab-containing chemotherapeutic regimen. Multivariate analysis indicated that HOXB9 expression was the most

significant independent predictive factors for PFS in this patient's cohort (HR=2.736; 95% CI=1.281-5.846; *P*=0.009) (Table 1). We did not demonstrate any correlation between HOXB9 expression and other clinico-pathologic variables in patients treated with a bevacizumab-containing chemotherapeutic regimen (Supplementary Table S3).

## DISCUSSION

In this study, we demonstrated for the first time that the transcription factor HOXB9 modulates the resistance of pancreatic and colorectal cancer to the anti-VEGF monoclonal antibody bevacizumab by orchestrating a complex network of alternative proinflammatory and proangiogenic secreted factors. Most importantly, to our knowledge this is the first study to candidate HOXB9 as potential biomarker for selecting patients with colorectal cancer for antiangiogenic therapy.

HOXB9 is potently emerging as one of the master regulator of angiogenesis. In a recent systematic analysis, miR-192 was identified as the most relevant miRNA for the control of angiogenesis in cancer. The potent anti-angiogenic activity of miR-192 depends on its ability to globally down regulate the expression of several proangiogenic factors, including Angptl2, CXCL1 and IL8, through the regulation of the transcription factors EGR1 and, importantly, HOXB9. Interestingly, delivery of miR-192 in multiple ovarian and renal tumor models by using a nanoliposomal platform significantly inhibited tumor angiogenesis, and resulted in a more profound antitumor effect compared with that observed with anti-VEGF treatment (24). Considering that our results demonstrate a key role for HOXB9 in sustaining resistance to anti-VEGF inhibition, it would be of primary interest the evaluation of the activity of miR-192 in combination with anti-VEGF treatment in preventing resistance, or as single agent treatment in models with acquired resistance to anti-VEGF strategies.

Two studies recently explored the role of HOXB9 in colorectal cancer models and patients showing contradictory results. In a first study evaluating a cohort of sixty-three cases of early colorectal cancer, patients with a high (3+) expression of HOXB9 at immunohistochemical analysis had a longer overall survival than did patients with moderate (2+) to no expression of this marker (25). Conversely, the second study (26) analyzed a different series of sixty-nine stage II and III colorectal cancers showing that increased HOXB9 mRNA expression levels were significantly associated with a shorter overall survival duration, and a poorly differentiated phenotype. In a subcohort of 39 cases of early colorectal cancer that at relapse were treated with chemotherapy and bevacizumab, increased HOXB9 mRNA

expression levels were significantly associated with a longer PFS and OS (26). Our present study explored the prognostic and predictive value of HOXB9 in a cohort of eighty-one advanced colorectal cancer patients by measuring the expression of this biomarker in a more relevant series of samples largely obtained at the diagnosis of metastatic disease. HOXB9 expression was correlated with the median PFS, a clinical endpoint that could be not corrupted by the effect of subsequent lines of therapy. Thus, no significant prognostic value was found for HOXB9 in the subcohort of patients treated with a first-line chemotherapeutic regimen non-containing bevacizumab. However, patients affected by an HOXB9-negative tumor had a significantly longer median PFS compared with those with an HOXB9-positve tumor in the subcohort of patients treated with a first-line chemotherapeutic regimen containing bevacizumab, suggesting for the first time a potential predictive value of this biomarker.

This study, however, had some limitations. In human-murine hybrid xenograft models bevacizumab could only block human tumor-derived VEGF with no effect on murine VEGF derived from host cells. However, this represent a common problem also for the different models in which bevacizumab has been developed in recent years in a large number of published preclinical studies leading, thus, to its clinical development and approval. We acknowledge that the recruitment of a stroma that produces murine VEGF is a possible mechanism of resistance to bevacizumab in tumor models. In this regard, the significance of our findings could be, indeed, an underestimation of what could actually happen in a fully human system. Moreover, the relevance of our analysis about the prognostic and predictive value of HOXB9 is limited by its retrospective design and the relatively small sample size. In this regard, a prospective randomized clinical trial about effectiveness of HOXB9 expression in selecting patients with colorectal cancer more likely to benefit from antiangiogenic drugs is warranted.

After more than 10 years since the approval of bevacizumab for the treatment of colorectal cancer, the identification of predictive biomarker for anti-VEGF therapies remains an unmeet need in clinical oncology. Our results reduce the complexity of numerous molecular mechanisms of resistance to the inhibition of VEGF by integrating them into the expression of a single transcription factor. The

usefulness of HOXB9 as an anti-VEGF treatment biomarker could be given also by the simple assessment and interpretation of its expression.

In conclusion, our study demonstrates for the first time HOXB9 as crucial transcription factor to sustain tumor resistance to bevacizumab. Silencing HOXB9 expression could be a promising approach to modulate this resistance. Our results candidate HOXB9 as novel biomarker to select patients with colorectal cancer more likely to benefit from antiangiogenic drugs.

**Acknowledgments**

Part of the work was performed at the Laboratorio Universitario di Ricerca Medica (LURM) Research Center, University of Verona. We thank Ms. Virginia Bonamico for data entry and administrative support. We thank Dr. Marzia Di Chio at the Department of Diagnostic and Public Health, University of Verona for technical execution of immunofluorescence analyses.

## REFERENCES


1. Ellis LM, Hicklin DJ. VEGF-targeted therapy: mechanisms of anti-tumour activity. Nat Rev Cancer **2008**;8(8):579-91.
2. Tortora G, Melisi D, Ciardiello F. Angiogenesis: a target for cancer therapy. Current pharmaceutical design **2004**;10(1):11-26.
3. Hurwitz H, Fehrenbacher L, Novotny W, Cartwright T, Hainsworth J, Heim W*, et al.* Bevacizumab plus irinotecan, fluorouracil, and leucovorin for metastatic colorectal cancer. N Engl J Med **2004**;350(23):2335-42 doi 10.1056/NEJMoa032691.
4. Hurwitz HI, Tebbutt NC, Kabbinavar F, Giantonio BJ, Guan ZZ, Mitchell L*, et al.* Efficacy and safety of bevacizumab in metastatic colorectal cancer: pooled analysis from seven randomized controlled trials. The oncologist **2013**;18(9):1004-12 doi 10.1634/theoncologist.2013-0107.
5. Van Cutsem E, Vervenne WL, Bennouna J, Humblet Y, Gill S, Van Laethem JL*, et al.* Phase III trial of bevacizumab in combination with gemcitabine and erlotinib in patients with metastatic pancreatic cancer. J Clin Oncol **2009**;27(13):2231-7.
6. Tamburrino A, Piro G, Carbone C, Tortora G, Melisi D. Mechanisms of resistance to chemotherapeutic and anti-angiogenic drugs as novel targets for pancreatic cancer therapy. Frontiers in pharmacology **2013**;4:56 doi 10.3389/fphar.2013.00056.
7. Jubb AM, Harris AL. Biomarkers to predict the clinical efficacy of bevacizumab in cancer. Lancet Oncol **2010**;11(12):1172-83 doi 10.1016/S1470-2045(10)70232-1.
8. Jain RK, Duda DG, Willett CG, Sahani DV, Zhu AX, Loeffler JS*, et al.* Biomarkers of response and resistance to antiangiogenic therapy. Nat Rev Clin Oncol **2009**;6(6):327-38 doi 10.1038/nrclinonc.2009.63.
9. Lambrechts D, Lenz HJ, de Haas S, Carmeliet P, Scherer SJ. Markers of response for the antiangiogenic agent bevacizumab. J Clin Oncol **2013**;31(9):1219-30 doi 10.1200/JCO.2012.46.2762.

10. van Beijnum JR, Nowak-Sliwinska P, Huijbers EJ, Thijssen VL, Griffioen AW. The great escape; the hallmarks of resistance to antiangiogenic therapy. Pharmacol Rev **2015**;67(2):441-61 doi 10.1124/pr.114.010215.
11. Sennino B, McDonald DM. Controlling escape from angiogenesis inhibitors. Nat Rev Cancer **2012**;12(10):699-709 doi 10.1038/nrc3366.
12. Clarke JM, Hurwitz HI. Understanding and targeting resistance to anti-angiogenic therapies. Journal of gastrointestinal oncology **2013**;4(3):253-63 doi 10.3978/j.issn.2078-6891.2013.036.
13. Carbone C, Moccia T, Zhu C, Paradiso G, Budillon A, Chiao PJ*, et al.* Anti-VEGF treatment-resistant pancreatic cancers secrete proinflammatory factors that contribute to malignant progression by inducing an EMT cell phenotype. Clinical cancer research : an official journal of the American Association for Cancer Research **2011**;17(17):5822-32 doi 10.1158/1078-0432.CCR-11-1185.
14. Carbone C, Tamburrino A, Piro G, Boschi F, Cataldo I, Zanotto M*, et al.* Combined inhibition of IL1, CXCR1/2, and TGFbeta signaling pathways modulates in-vivo resistance to anti-VEGF treatment. Anti-cancer drugs **2016**;27(1):29-40 doi 10.1097/CAD.0000000000000301.
15. Shah N, Sukumar S. The Hox genes and their roles in oncogenesis. Nature reviews **2010**;10(5):361-71 doi 10.1038/nrc2826.
16. Nguyen DX, Chiang AC, Zhang XH, Kim JY, Kris MG, Ladanyi M*, et al.* WNT/TCF signaling through LEF1 and HOXB9 mediates lung adenocarcinoma metastasis. Cell **2009**;138(1):51-62 doi 10.1016/j.cell.2009.04.030.
17. Chiba N, Comaills V, Shiotani B, Takahashi F, Shimada T, Tajima K*, et al.* Homeobox B9 induces epithelial-to-mesenchymal transition-associated radioresistance by accelerating DNA damage responses. Proc Natl Acad Sci U S A **2012**;109(8):2760-5 doi 10.1073/pnas.1018867108.

18. Hayashida T, Takahashi F, Chiba N, Brachtel E, Takahashi M, Godin-Heymann N*, et al.* HOXB9, a gene overexpressed in breast cancer, promotes tumorigenicity and lung metastasis. Proc Natl Acad Sci U S A **2010**;107(3):1100-5 doi 10.1073/pnas.0912710107.

19. Seki H, Hayashida T, Jinno H, Hirose S, Sakata M, Takahashi M*, et al.* HOXB9 expression promoting tumor cell proliferation and angiogenesis is associated with clinical outcomes in breast cancer patients. Ann Surg Oncol **2012**;19(6):1831-40 doi 10.1245/s10434-012-2295-5.

20. Melisi D, Xia Q, Paradiso G, Ling J, Moccia T, Carbone C*, et al.* Modulation of pancreatic cancer chemoresistance by inhibition of TAK1. J Natl Cancer Inst **2011**;103(15):1190-204 doi 10.1093/jnci/djr243.

21. Piro G, Carbone C, Cataldo I, Di Nicolantonio F, Giacopuzzi S, Aprile G*, et al.* An FGFR3 autocrine loop sustains acquired resistance to trastuzumab in gastric cancer patients. Clin Cancer Res **2016** doi 10.1158/1078-0432.CCR-16-0178.

22. Melisi D, Ossovskaya V, Zhu C, Rosa R, Ling J, Dougherty PM*, et al.* Oral poly(ADP-ribose) polymerase-1 inhibitor BSI-401 has antitumor activity and synergizes with oxaliplatin against pancreatic cancer, preventing acute neurotoxicity. Clin Cancer Res **2009**;15(20):6367-77 doi 10.1158/1078-0432.CCR-09-0910.

23. Medico E, Russo M, Picco G, Cancelliere C, Valtorta E, Corti G*, et al.* The molecular landscape of colorectal cancer cell lines unveils clinically actionable kinase targets. Nature communications **2015**;6:7002 doi 10.1038/ncomms8002.

24. Wu SY, Rupaimoole R, Shen F, Pradeep S, Pecot CV, Ivan C*, et al.* A miR-192-EGR1-HOXB9 regulatory network controls the angiogenic switch in cancer. Nature communications **2016**;7:11169 doi 10.1038/ncomms11169.

25. Zhan J, Niu M, Wang P, Zhu X, Li S, Song J*, et al.* Elevated HOXB9 expression promotes differentiation and predicts a favourable outcome in colon adenocarcinoma patients. Br J Cancer **2014**;111(5):883-93 doi 10.1038/bjc.2014.387.

26. Hoshino Y, Hayashida T, Hirata A, Takahashi H, Chiba N, Ohmura M*, et al.* Bevacizumab terminates homeobox B9-induced tumor proliferation by silencing microenvironmental communication. Molecular cancer **2014**;13:102 doi 10.1186/1476-4598-13-102.

**Table 1. Univariate and multivariate analysis for PFS in bevacizumab treated colorectal cancer patients**

| Characteristic | Univariate | | Multivariate | |
|---|---|---|---|---|
| | **HR (95% CI)** | ***P*** | **HR (95% CI)** | ***P*** |
| **Age** | | | | |
| <69 years | | | | |
| >69 years | 1.439 (0.812 - 2.548) | 0.212 | | |
| **Primary tumor size (T)** | | | | |
| T1-2 | | | | |
| T3-4 | 2.294 (1.065 - 4.944) | 0.034 | 2.414 (1.079 - 5.411) | 0.032 |
| **ECOG PS** | | | | |
| PS 0 | | | | |
| PS 1-2 | 1.939 (1.062 - 3.540) | 0.031 | 1.707 (0.915 - 3.186) | 0.093 |
| **Time of metastasis occurrence** | | | | |
| Metachronous | | | | |
| Synchronous | 1.842 (0.986 - 3.441) | 0.055 | | |
| **Mutational status** | | | | |
| B-RAF/N-RAS Wild-type | | | | |
| B-RAF/N-RAS Mutated | 3.019 (1.166 - 7.814) | 0.023 | 2.139 (0.803 - 5.701) | 0.128 |
| **Liver metastasis** | | | | |
| No | | | | |
| Yes | 1.518 (0.820 - 2.811) | 0.184 | | |
| **KRAS status** | | | | |
| Wild-type | | | | |
| Mutated | 0.601 (0.331 - 1.092) | 0.094 | | |
| **HOXB9, n (%)** | | | | |
| Negative | | | | |
| Positive | 2.037 (1.006 - 4.125) | 0.048 | 2.552 (1.180 - 5.518) | 0.017 |

*HR* hazard ratio; *CI* confidence interval; *PS* performance status

**Figure Legends**

**Figure 1.** HOXB9 is overexpressed and activated in bevacizumab-resistant FGBR pancreatic cancer models. **A**) Twenty athymic nude mice bearing orthotopic luc-GFP+ bevacizumab-sensitive COLO357FG, or bevacizumab-resistant FGBR pancreatic tumors were randomly assigned to 4 groups (n= 5 per group) to receive 100 μg of either bevacizumab or saline (vehicle) i.p. twice a week. Differences among survival duration of mice in each group were determined by log-rank test; **B**) Western blot analysis for the expression of HOXB9 in cytosolic and nuclear compartment from COLO357FG and FGBR cell lines; **C**) Representative images showing HOXB9 protein expression (red) by confocal microscopy, nuclei were stained with Hoechst 33342 (blue). Fluorescence intensity analysis was performed by ImageJ software and bars represent mean ± 95% CI from analysis of 8 separate high power field images; *** P<0.001, ** P<0.05, by two-tailed unpaired Student's t-test; **D**) Electrophoretic Mobility Shift Assay analysis for DNA-binding activity of HOXB9; **E**) Immunohistochemistry analysis for the expression of HOXB9 in COLO357FG and FGBR tumor-bearing mice; **F**) Multiplex bead-based human cytokine assay for serum detection of circulating factors in COLO357FG and FGBR tumor bearing mice. Mean and 95% CI in ng/mL are shown. *** P<0.001, ** P<0.05, by two-tailed unpaired Student's t-test; **G**) Western blotting analysis for the expression of HOXB9 in FGBR control cells and in the same cells transduced with lentiviruses expressing shRNA or with scramble sequence as control; **H**) DNA affinity precipitation assay of HOXB9 in COLO357FG and FGBR, and in FGBR expressing shHOXB9 or a scramble sequence as control; **I**) Western blot analysis for the expression of EMT markers E-Cadherin and vimentin in FGBR, and in FGBR expressing shHOXB9 or a scramble sequence as control; γ-tubulin was used as loading control; **J)** Levels of cancer cell migration in FGBR, and in FGBR expressing shHOXB9, a scramble sequence or control. Results are presented as percentages of the total distances between the wound edges enclosed by cancer cells. The mean values and 95% confidence intervals from three independent

experiments performed in quadruplicate are shown. Photographs of the wound area were taken using phase contrast microscopy immediately and 36 h after the incision.

**Figure 2.** Silencing HOXB9 Modulates Anti-VEGF Resistance In Pancreatic Cancer Models. **A**) Multiplex bead-based human cytokine assay for serum detection of circulating factors in FGBR cancer tumor bearing mice. Mean and 95% confidence intervals (CI) in ng/mL are shown. *** $P<0.001$, **$P<0.05$ by two-tailed unpaired Student's t-test; **B**) Hematoxylin-eosin staining and immunohistochemistry analysis for HOXB9 and E-cadherin and Vimentin expression in nude mice bearing FGBR cells expressing shHOXB9 or a scramble sequence as control; **C**) Representative images and relative vasculature in FGBR expressing shHOXB9 or a scramble sequence as control tumor-bearing mice; **D**) Twenty athymic nude mice bearing subcutaneous $FGBR^{shHOXB9}$ or $FGBR^{scramble}$ pancreatic tumors were randomly assigned (n=5 per group) to receive 100 μg of either bevacizumab or saline (vehicle) i.p. twice a week. Tumor size was measured with a caliper IVIS 100 imaging system. Mean tumor volume and 95% confidence intervals (CI) in $mm^3$ are shown, $P<0.001$ by Student's t-test. **E)** Differences among survival duration of mice in each group were determined by log-rank test.

**Figure 3.** HOXB9 sustains resistance to anti-VEGF therapy in colorectal cancer models. **A**) Western blot analysis for the expression of HOXB9, γ-tubulin was used as loading control; **B**) representative images showing HOXB9 protein expression (red) by confocal microscopy, nuclei were stained with Hoechst 33342 (blue). Fluorescence intensity analysis was performed by ImageJ software and bars represent mean ± 95% CI from analysis of 8 separate high power field images. *** $P<0.001$, ** $P<0.05$, by two-tailed unpaired Student's t-test; **C**) Gene expression levels of differentially secreted genes in colorectal cancer cells. In the heat map shown in this figure, the logarithms of the gene expression levels are shown in colors (green= decreased expression, red= increased expression); **D**) Western blot analysis for the expression of EMT markers E-Cadherin and vimentin in

whole protein extracts; g-tubulin was used as loading control; **E**) Multiplex bead-based human cytokine assay for serum detection of circulating factors in colorectal cancer tumor bearing mice; **F**) Hematoxylin-eosin staining and immunohistochemistry analysis for the expression of HOXB9 and E-cadherin and Vimentin in nude mice bearing colorectal cancer cell lines; **G**) forty athymic nude mice bearing subcutaneous HOXB9-positive LIM2099 and MDST8 or HOXB9-negative GP5D and CCK81 colorectal tumors were randomly assigned (n=5 per group) to receive 100 μg of either bevacizumab or saline (vehicle) i.p. twice a week. The day of sacrifice was considered the day of death from disease for the purpose of survival evaluation. Differences among survival duration in each group were determined by log-rank test.

**Figure 4.** Silencing HOXB9 modulates anti-VEGF resistance in colorectal cancer models. **A**) Western blot analysis for the expression of HOXB9 in MDST8 control cells and in the same cells transduced with two lentiviruses expressing HOXB9-specific small hairpin RNA (shHOXB9 and shHOXB9a) or with scramble sequence as control; g-tubulin was used as loading control; **B**) Levels of cancer cell migration in MDST8, and MDST8 expressing shHOXB9 or a scramble sequence as control. Results are presented as percentages of the total distances between the wound edges enclosed by cancer cells. The mean values and 95% confidence intervals from three independent experiments performed in quadruplicate are shown. Photographs of the wound area were taken using phase contrast microscopy immediately and 36 h after the incision; **C**) Multiplex bead-based human cytokine assay for serum detection of circulating factors in colorectal cancer tumor bearing mice. Mean and 95% CI in ng/mL are shown. *** $P<0.001$, ** $P<0.05$, by two-tailed unpaired Student's t-test; **D**) Hematoxylin-eosin staining and immunohistochemistry analysis for the expression of HOXB9 and E-cadherin and Vimentin in nude mice bearing MDST8 cells expressing shHOXB9 or a scramble sequence as control; **E**) Representative images and relative vasculature in MDST8 expressing shHOXB9 or a scramble sequence as control tumor-bearing mice; **F**) twenty athymic nude mice bearing subcutaneous MDST8 HOXB9 stably silenced or scramble cells were randomly assigned (n=5

per group) to receive 100 μg of either bevacizumab or saline (vehicle) i.p. twice a week. Mean tumor volume and 95% CI in $mm^3$ are shown, P<0.001 by Student's t-test; **G)** Differences among survival duration of mice in each group were determined by log-rank test.

**Figure 5.** HOXB9 expression is an independent predictive factor for progression free survival in metastatic colorectal cancer patients treated with bevacizumab. Kaplan-Meier plots of Progression free survival (PFS) by HOXB9 expression in no-bevacizumab treated **A**) and bevacizumab treated **B**) patients. All *P* values were calculated by the log rank test; **C**) Paraffin-embedded tumor sections stained immunohistochemically with antibodies against HOXB9. Statistical analyses are shown in table 1.

# Figure 1

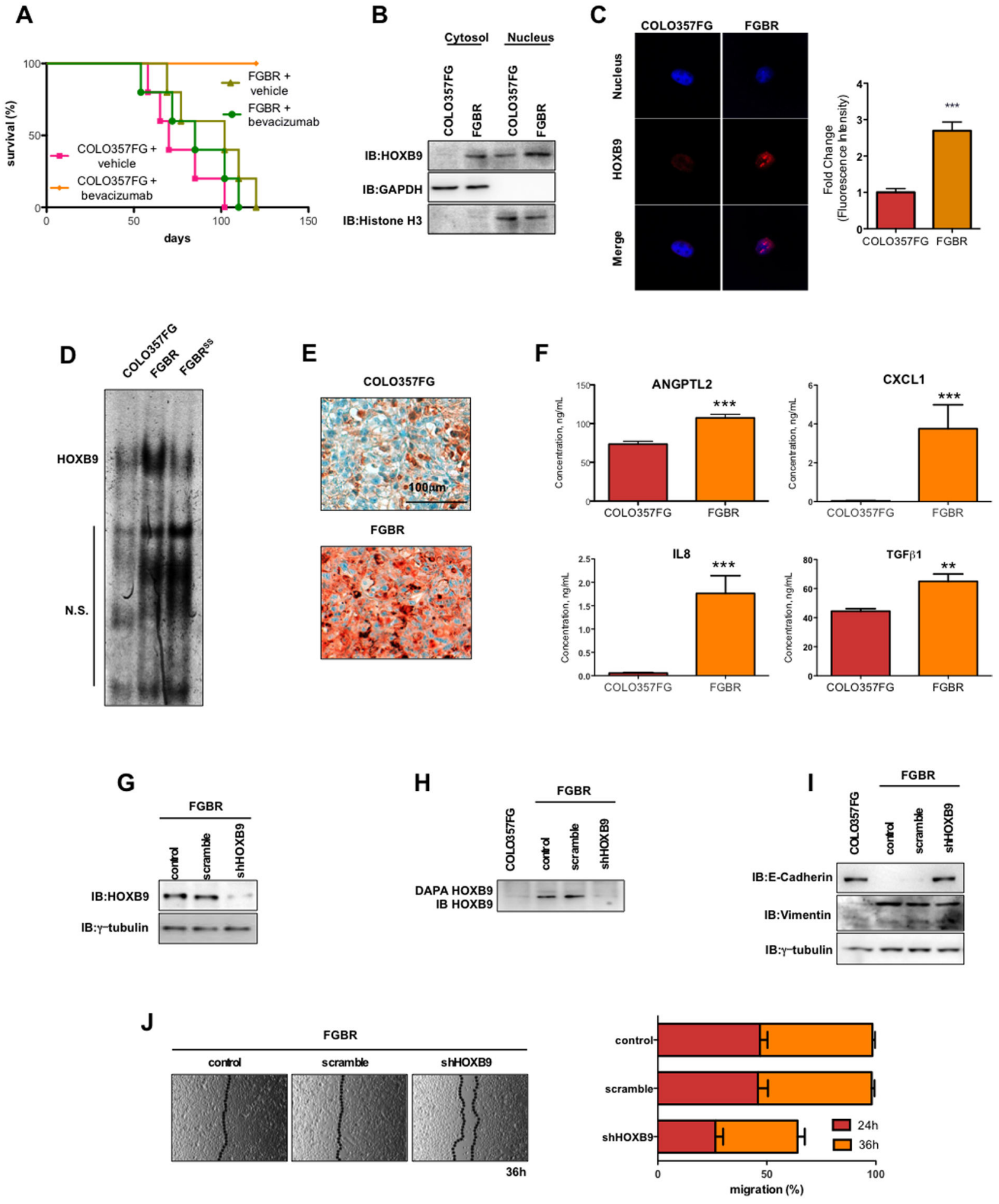
A
survival (%)
days
FGBR + vehicle
FGBR + bevacizumab
COLO357FG + vehicle
COLO357FG + bevacizumab
B
Cytosol
Nucleus
COLO357FG
FGBR
IB:HOXB9
IB:GAPDH
IB:Histone H3
C
COLO357FG
FGBR
Nucleus
HOXB9
Merge
Fold Change (Fluorescence Intensity)
D
COLO357FG
FGBR
FGBRSS
HOXB9
N.S.
E
COLO357FG
FGBR
100μm
F
ANGPTL2
CXCL1
IL8
TGFβ1
Concentration, ng/mL
G
FGBR
control
scramble
shHOXB9
IB:HOXB9
IB:γ-tubulin
H
FGBR
COLO357FG
control
scramble
shHOXB9
DAPA HOXB9
IB HOXB9
I
FGBR
COLO357FG
control
scramble
shHOXB9
IB:E-Cadherin
IB:Vimentin
IB:γ-tubulin
J
FGBR
control
scramble
shHOXB9
36h
control
scramble
shHOXB9
24h
36h
migration (%)

# Figure 2

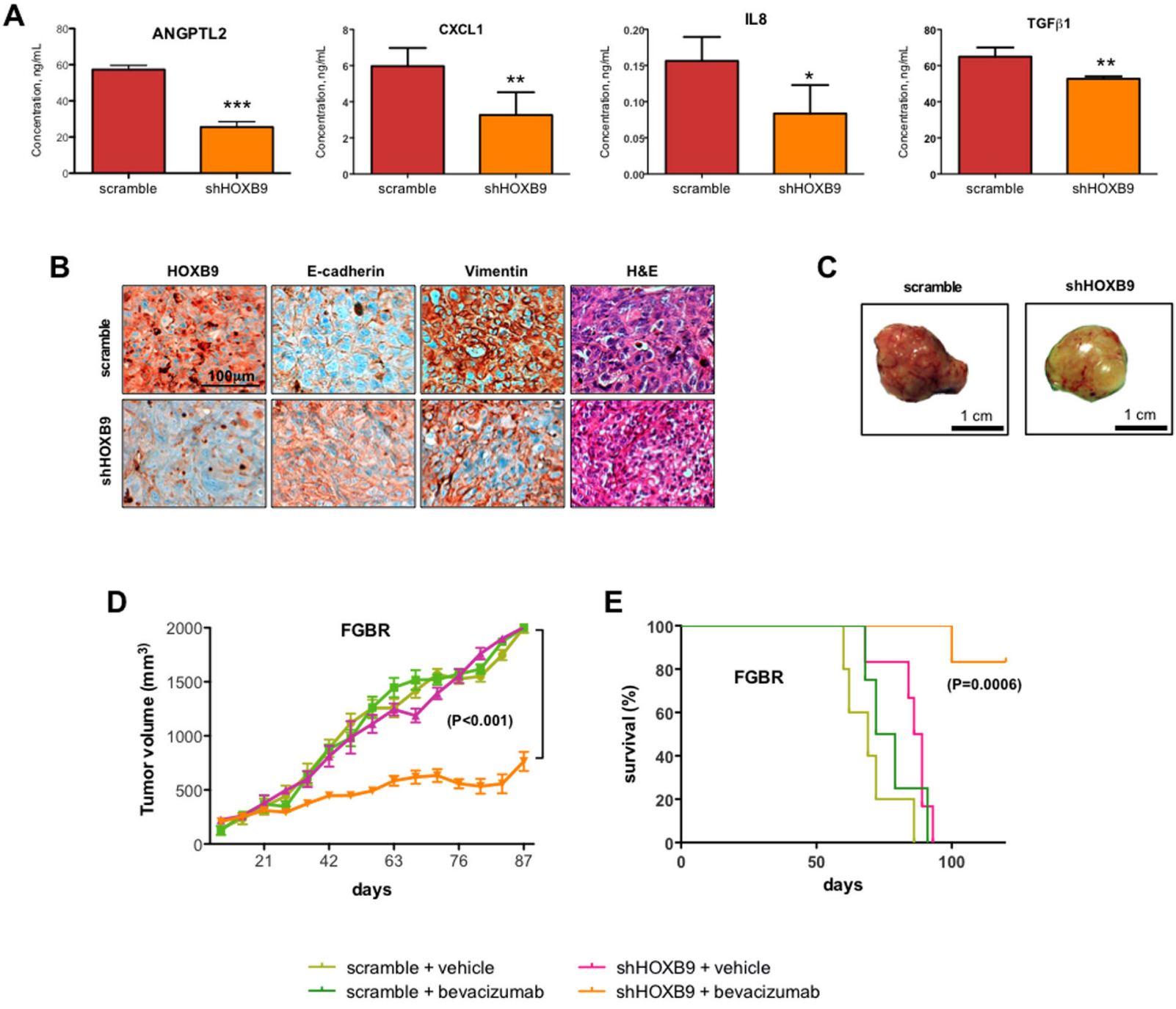
A
ANGPTL2
CXCL1
IL8
TGFβ1
Concentration, ng/mL
scramble
shHOXB9
***
**
*
**
B
HOXB9
E-cadherin
Vimentin
H&E
scramble
shHOXB9
100μm
C
scramble
shHOXB9
1 cm
1 cm
D
FGBR
Tumor volume (mm3)
days
(P<0.001)
E
FGBR
survival (%)
days
(P=0.0006)
scramble + vehicle
scramble + bevacizumab
shHOXB9 + vehicle
shHOXB9 + bevacizumab

# Figure 3

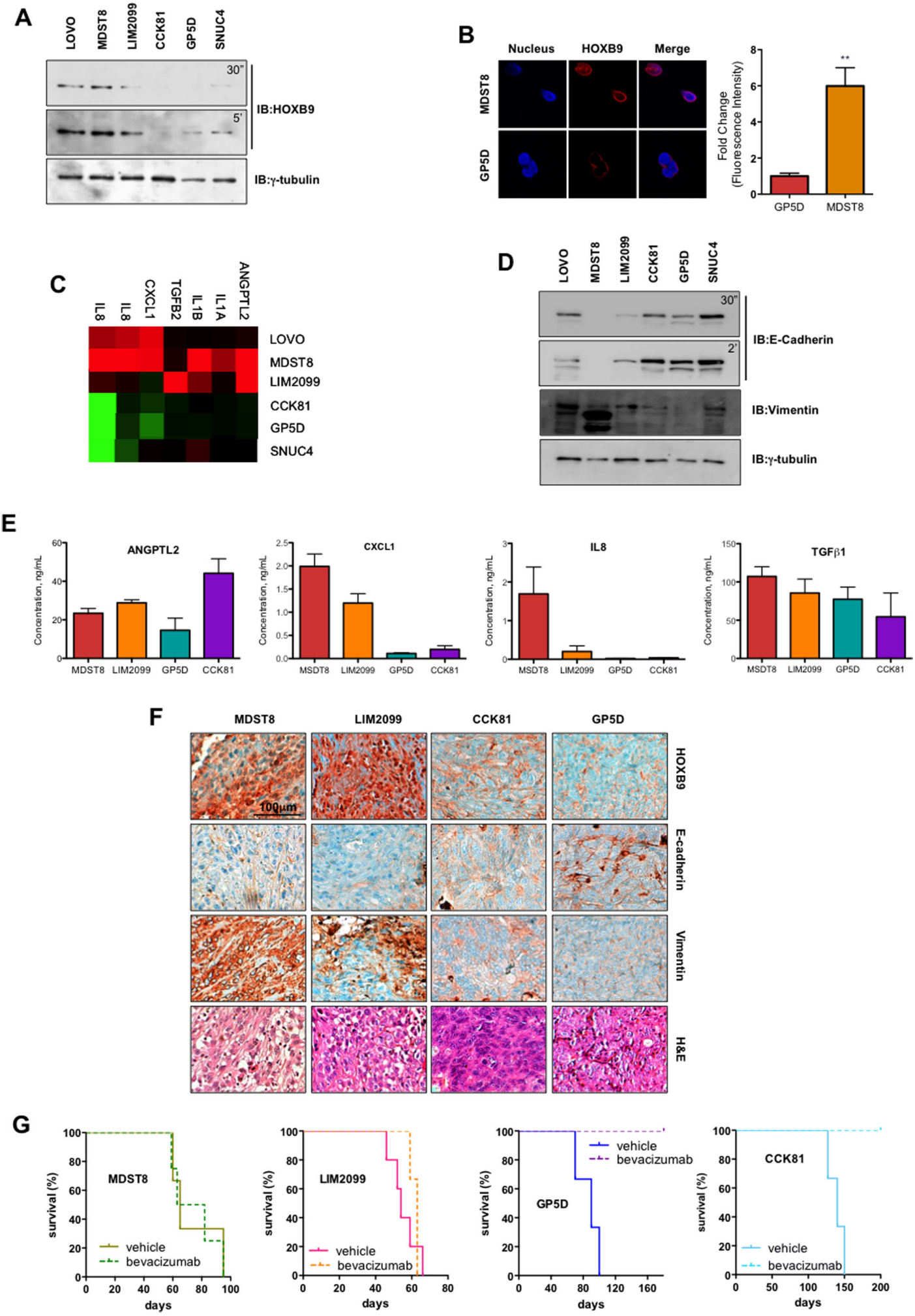
A
LOVO
MDST8
LIM2099
CCK81
GP5D
SNUC4
30"
5'
IB:HOXB9
IB:γ-tubulin
B
Nucleus
HOXB9
Merge
MDST8
GP5D
Fold Change (Fluorescence Intensity)
**
GP5D
MDST8
C
IL8
IL8
CXCL1
TGFB2
IL1B
IL1A
ANGPTL2
LOVO
MDST8
LIM2099
CCK81
GP5D
SNUC4
D
LOVO
MDST8
LIM2099
CCK81
GP5D
SNUC4
30"
2'
IB:E-Cadherin
IB:Vimentin
IB:γ-tubulin
E
ANGPTL2
CXCL1
IL8
TGFβ1
Concentration, ng/mL
MDST8
LIM2099
GP5D
CCK81
F
MDST8
LIM2099
CCK81
GP5D
100μm
HOXB9
E-cadherin
Vimentin
H&E
G
MDST8
LIM2099
GP5D
CCK81
survival (%)
days
vehicle
bevacizumab

# Figure 4

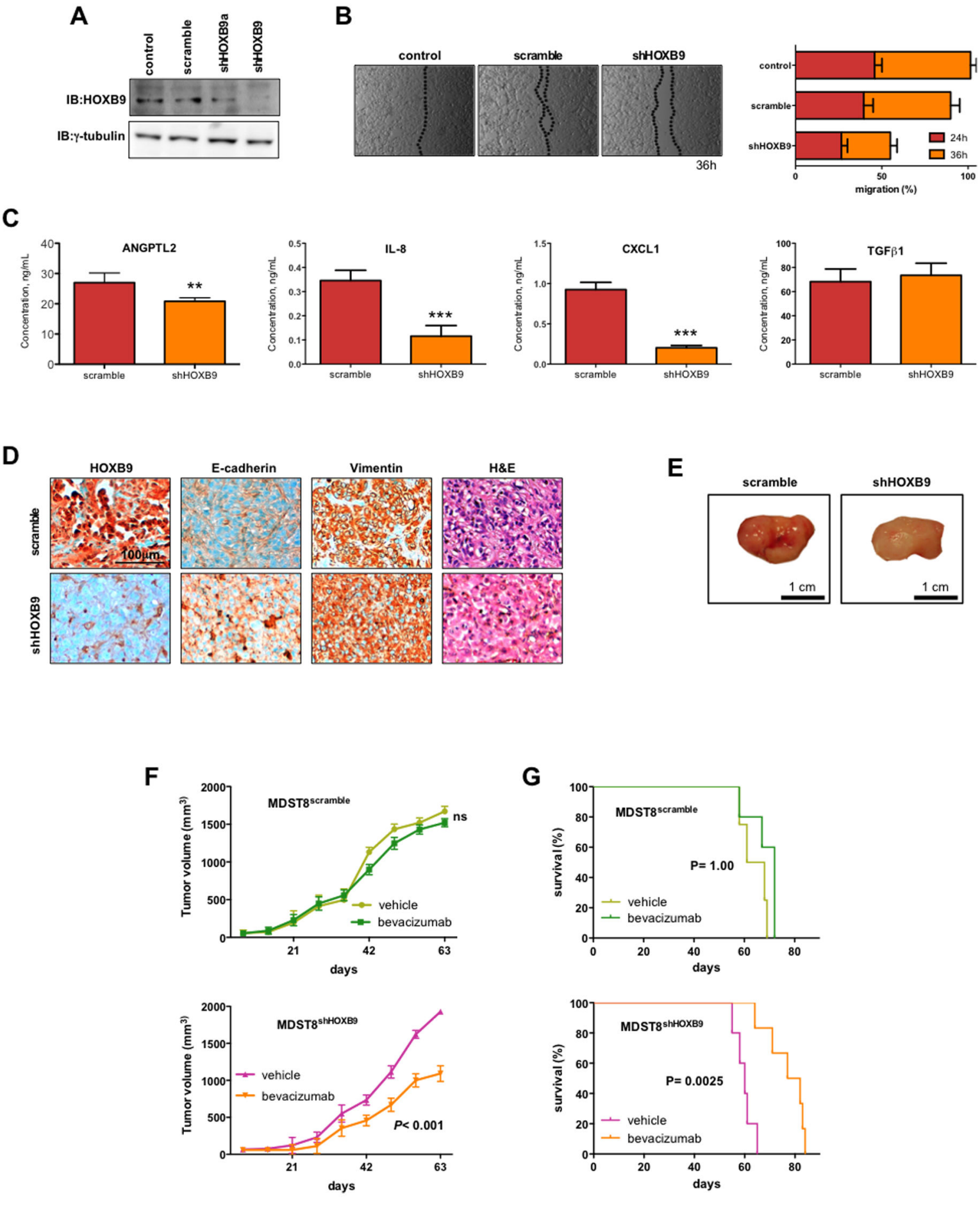
A
control
scramble
shHOXB9a
shHOXB9
IB:HOXB9
IB:γ-tubulin
B
control
scramble
shHOXB9
36h
control
scramble
shHOXB9
24h
36h
0
50
100
migration (%)
C
ANGPTL2
Concentration, ng/mL
**
scramble
shHOXB9
IL-8
***
CXCL1
***
TGFβ1
D
HOXB9
E-cadherin
Vimentin
H&E
scramble
shHOXB9
100μm
E
scramble
shHOXB9
1 cm
1 cm
F
MDST8scramble
Tumor volume (mm3)
ns
vehicle
bevacizumab
days
MDST8shHOXB9
P< 0.001
G
MDST8scramble
survival (%)
P= 1.00
MDST8shHOXB9
P= 0.0025

Figure 5

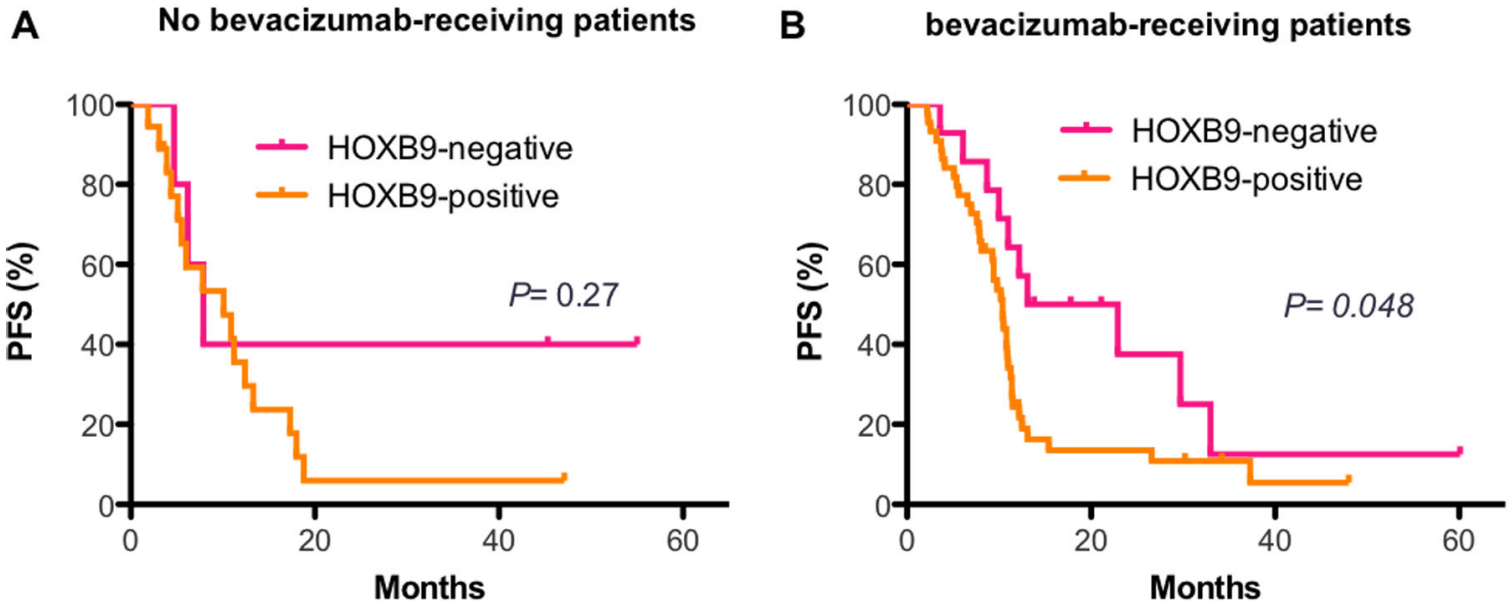
A
No bevacizumab-receiving patients
PFS (%)
100
80
60
40
20
0
HOXB9-negative
HOXB9-positive
P= 0.27
0
20
40
60
Months
B
bevacizumab-receiving patients
PFS (%)
HOXB9-negative
HOXB9-positive
P= 0.048
Months

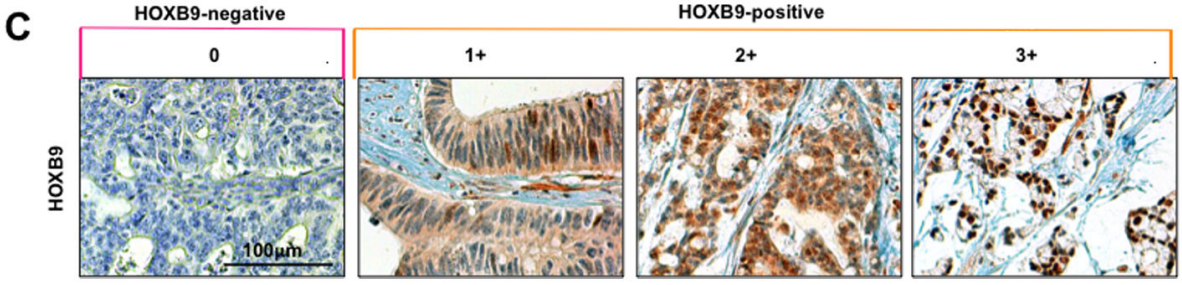
C
HOXB9-negative
HOXB9-positive
0
1+
2+
3+
HOXB9
100μm

**Carbone C. et al. Supplementary Methods**

## Cell Lines

The cancer cell lines COLO357FG was obtained from the laboratory of Prof. Paul J. Chiao (MD Anderson Cancer Center). Human colorectal cancer cell line CCK81 was purchased from the Japanese Collection of Research Bioresources Cell Bank. GP5D and MDST8 cells were obtained from the European Collection of Authenticated Cell Cultures (ECACC). SNUC4 cell line was retrieved from the Korean Cell Line Bank (KCLB), LOVO cells were purchased from the ATCC through a local distributor (LGC Standards, Sesto San Giovanni, Italy). LIM2099 cells were a kind gift of Dr. F. Walker, Ludwig Institute for Cancer Research, Melbourne-Parkville Branch, Australia. Cells were daily checked by morphology and routinely tested to be Mycoplasma free by PCR assay.

## Generation of HOXB9 knockdown cell lines

$RFP^+$ HOXB9-$shRNA^+$ cell lines were obtained by lentiviral infection. Briefly, lentivirus was produced by transient cotransfection into the human 293T cell line with lentiviral helper plasmids (packaging vectors pMDLg/pRRE and pRSV/Rev, and envelope vector pMD2/VSVG) and RFP HOXB9 shRNA lentivector (sigma-Aldrich) using LT1-mirus according to manufacturer method. 18 hours later, growth media (DMEM containing 10% Fetal Bovine Serum and 1% penicillin/streptomycin) were changed. Lentiviral supernatant was harvested at 48 h and 72 h post transfection and filtered through a 0.45-μm filter. Lentiviral supernatants were concentrated 20- fold by ultracentrifugation at 4°C for 10 h at 10,000 g. Harvested lentiviruses were stored at -80°C. Pancreatic cancer cell lines FGBR and colorectal cancer cell lines MDST8 were infected by adding thawed lentivirus-containing supernatant. To assess the activity of virus encoding the RFP reporter gene, RFP expression was assessed by fluorescence microscopy (Axiovert, Zeiss, Oberkochen, Germany).

## Decoy oligodeoxynucleotides

FGBR pancreatic cancer cell line and MSDT8 colorectal cancer cell line were transfected with double-strand phosphorothioate oligodeoxynucleotides containing the HOXB9 binding site (ODNHOXB9) and a control sequence (ODNmut) at different concentration using LT1-mirus as described by the manufacturer's instructions. ODNHOXB9 was used at 1 and 2 μM and ODNmut at 2 μM.

**Wound Healing Migration assay**

Cell lines were seeded to 90% of confluence in 100 mm cell culture dishes. After 24 hours cells a straight scratch was made using a pipette tip to simulate a wound. The cells were washed gently with cold PBS 1X and rinsed with fresh medium. Photographs at five different points at least were taken immediately and after 24 and 36 hours of culture.

**RNA Isolation and Quantitative RT-PCR Assay**

Total RNA was obtained from cells using Trizol reagent (Invitrogen, Carlsbad, CA, USA) and following the procedures outlined by the supplier. The quality of RNA was determined by electrophoresis on agarose gel and staining with ethidium bromide, the 18S and 28S bands were visualized by ultraviolet light. Total RNA was quantified by absorbance at 260 nm. Reverse transcription was performed using the High Capacity Reverse Transcription Kit (Qiagen, Venlo, Netherlands). The cDNA obtained was evaluated for Real-Time PCR with ABI Prism 7900 HT Sequence Detection System (Applied Biosystems, Foster City, CA, USA) using specific primer and SYBR Green. QuantiTect Primer Assays (Qiagen, Venlo, Netherlands) were used to quantify cDNA levels of CDH1, VIM, ANGPTL2, CXCL1, IL1A, IL1B, CXCL8, VEGFa, TGFβ2 and β-Actin. Gene expression was calculated using $2^{-\Delta\Delta}$CT method and normalized to β-actin expression.

**Xenograft Model in Nude Mice**

Tumor bearing mice were randomly assigned (n=5 per group) to receive 100 μg of bevacuzumab i.p. twice a week or saline as a control. In mice bearing orthotopic xenografts, tumor growth was quantified weekly on the basis of bioluminescence emitted by the tumor cells as the

sum of all detected photons within the region of the tumor per second using a cryogenically cooled IVIS 100 imaging system coupled with a data-acquisition computer running the Living Image software program (Xenogen, Hopkinton, MA). In mice bearing heterotopic xenografts, the tumor size was measured with a caliper by the modified ellipsoid formula (π/6) x AB2 where A is the longest and B is the shortest perpendicular axis of an assumed ellipsoid corresponding to tumor mass. When at least three of the five mice in a treatment group presented with bulky disease, the median survival duration for that group was considered to have been reached. At the median survival duration of the control group, the tumor growth in mice in all groups was evaluated. The mice were euthanized using carbon dioxide inhalation when evidence of advanced bulky disease developed or at cut-off volume of 2 $cm^3$, which was considered the day of death for the purpose of survival evaluation. Animal study was approved by the local ethics committee.

**Immunohistochemistry**

Three-micrometer thick tumor sections were stained with primary rabbit anti-human antibodies: anti-HOXB9 rabbit polyclonal antibody (ab66765), anti-E-Cadherin monoclonal antibody (ab40772) and anti-CD11b monoclonal antibody (ab52478) were from Abcam, Cambridge, UK; mouse monoclonal anti-vimentin (HPA001762) was from Sigma Saint Louis, MO. Staining was done on an automated stainer system (BenchMark ULTRA – Ventana Medical Systems) using the ultraView DAB Detection Kit (Ventana Medical Systems). The analysis of immunostaining was assessed evaluating separately the percentage of positive tumor cells (nuclear positivity) and their staining intensity (- negative, + weak, ++ moderate, +++ intense).

**Statistical Analysis**

The results of in vitro proliferation and migration assays, Luminex xMAP, ELISA, and RT-PCR were analyzed for statistical significance of differences by two-tailed unpaired Student's t-test and are expressed as means and 95% confidence intervals (CI). Statistical significance of differences in tumor growth was determined by the Mann–Whitney test. Differences in survival duration were determined using a log-rank test (Mantel Cox's test). A p value less than 0.05 indicated statistical

significance. For patient cohort analysis, progression-free survival (PFS) was calculated as the period from the first day of treatment to the date of tumor progression. PFS curves were drawn by Kaplan-Meier estimates and compared by log rank test. Univariate and multivariate analyses of PFS, with stepwise variable selection, were conducted by Cox's proportional hazard regression models. Multivariate analysis was conducted using the variables that were significant in univariate analysis ($p \leq 0.05$). The relationship between HOXB9 expression and clinic-pathological characteristics was examined using the $\chi 2$ method for linear trend.

All statistical analyses of in vitro assays were performed using GraphPad Prism software version 4.0c for Macintosh (GraphPad Software, San Diego, CA). Statistical analysis for patient cohort was performed using SPSS 24.0 statistical software (SPSS, Inc., Chicago, IL).

**Supplementary Table S1. Patient characteristics**

| | All patients (n=81) | Bevacizumab treated patients (n=58) | Bevacizumab untreated patients (n=23) |
|---|---|---|---|
| **Age, median (range)** | 69 (25-86) | 69 (25-84) | 69 (48-86) |
| **Sex, n (%)** | | | |
| M | 45 (55.56) | 31 (53.45) | 14 (60.87) |
| F | 36 (44.44) | 27 (46.55) | 9 (39.13) |
| **PS ECOG, n (%)** | | | |
| 0 | 52 (64.20) | 39 (67.24) | 13 (56.52) |
| 1 | 27 (33.33) | 17 (29.31) | 10 (43.48) |
| 2 | 1 (1.23) | 1 (1.72) | 0 |
| na | 1 (1.23) | 1 (1.72) | 0 |
| **Stage at diagnosis, n (%)** | | | |
| I | 2 (2.47) | 2 (3.45) | 0 |
| II | 10 (12.35) | 6 (10.34) | 4 (17.39) |
| III | 22 (27.16) | 18 (31.03) | 4 (17.39) |
| IV | 46 (56.79) | 31 (53.45) | 15 (65.22) |
| na | 1 (1.23) | 1 (1.72) | 0 |
| **Site of primary tumor, n (%)** | | | |
| Left Colon | 29 (35.80) | 20 (34.48) | 9 (39.13) |
| Right Colon | 35 (43.21) | 25 (43.10) | 10 (43.48) |
| Colon NOS | 2 (2.47) | 2 (3.45) | 0 |
| Rectum | 15 (18.52) | 11 (18.97) | 4 (17.39) |
| **Site of metastasis, n (%)** | | | |
| Liver | 53 (65.43) | 37 (63.79) | 16 (69.57) |
| Lung | 26 (32.10) | 18 (31.03) | 8 (34.78) |
| Node | 23 (28.40) | 20 (34.48) | 3 (13.04) |
| Peritoneum | 24 (29.63) | 16 (27.59) | 8 (34.78) |
| Bone | 2 (2.47) | 2 (3.45) | 0 |
| Other | 13 (16.05) | 9 (15.52) | 4 (17.39) |
| **KRAS status, n (%)** | | | |
| Wild-type | 25 (30.86) | 19 (32.76) | 6 (26.09) |
| Mutated | 56 (69.14) | 39 (67.24) | 17 (73.91) |
| **NRAS status, n (%)** | | | |
| Wild-type | 72 (88.89) | 51 (87.93) | 21 (91.30) |
| Mutated | 5 (6.17) | 5 (8.62) | 0 |
| na | 4 (4.94) | 2 (3.45) | 2 (8.70) |
| **BRAF status, n (%)** | | | |
| Wild-type | 78 (96.30) | 56 (96.55) | 22 (95.65) |
| Mutated | 3 (3.70) | 2 (3.45) | 1 (4.35) |
| **Primary tumor size (T), n (%)** | | | |
| T1 | 1 (1.23) | 1 (1.72) | 0 |
| T2 | 10 (12.35) | 10 (17.24) | 0 |
| T3 | 57 (70.37) | 38 (65.51) | 19 (82.6) |
| T4 | 12 (14.81) | 8 (13.79) | 4 (17.39) |
| na | 1 (1.23) | 1 (1.72) | 0 |
| **Time of metastasis occurrence, n (%)** | | | |
| metachronous | 30 (37.03) | 22 (37.93) | 8 (34.78) |
| synchronous | 51 (62.96) | 36 (62.06) | 15 (65.21) |
| **HOXB9, n (%)** | | | |
| Negative | 19 (23.46) | 14 (24.14) | 5 (21.74) |
| Positive | 62 (76.54) | 44 (75.86) | 18 (78.26) |

**Supplementary Table S2.** Compliance with REMARK guidelines

| | |
|---|---|
| **Introduction** | |
| | Marker analyzed is HOXB9.<br>Objectives; to determine whether HOXB9 is predictive for benefit from bevacizumab-containing first-line chemotherapeutic treatment.<br>Hypotheses; HOXB9 positivity is associated with poor response to bevacizumab treatment. |
| **Materials and Methods** | |
| - Patients | Metastatic colorectal cancer patients treated or not with a bevacizumab-containing first-line chemotherapeutic regimen. |
| - Specimen characteristics | Paraffin-embedded tissue from biopsies specimens obtained at the diagnosis of metastatic colorectal cancer with at least 80% of tumor cellularity. |
| - Assay method | IHC analysis was assessed evaluating nuclear positivity and staining intensity (- negative, + weak, ++ moderate, +++ intense). IHC analysis was performed blinded to the study endpoint. Detailed protocol described in Materials and Methods section. |
| - Study design | Retrospective analysis of paraffin-embedded samples from patients treated or not with a bevacizumab-containing first-line chemotherapeutic regimen collected between October 2004 and July 2015. The median follow-up was 23.7 months.<br>Clinical end-point, progression free survival (PFS).<br>Sample size determined by the availability of tissue. |
| - Statistical methods | Survival curves of patients in each treatment arm stratified according to HOXB9 levels were drawn by Kaplan-Meier estimates and compared by log rank test.<br>Multivariate analysis of PFS, with stepwise variable selection, was conducted by Cox's proportional hazard regression model to assess the independent predictive value of HOXB9.<br>Relationship between HOXB9 expression and clinic-pathological characteristics was examined using the $\chi 2$ method for linear trend. |
| **Results** | |
| - Data | Patient's characteristics reported in supplementary Table S1. |
| - Analysis and presentation | Univariate and multivariate analyses results reported in Table 1.<br>Correlation between HOXB9 expression and clinic-pathologic characteristic displayed in supplementary Table S3.<br>Kaplan–Meier survival curves for effect of HOXB9 expression on progression free survival in Figure 5. |
| **Discussion** | |
| | HOXB9 had no prognostic value in patients treated with a first-line chemotherapeutic regimen non-containing bevacizumab. However, patients affected by an HOXB9-negative tumor had a significantly longer PFS compared with those with an HOXB9-positive tumor if treated with a first-line regimen containing bevacizumab. Study limited by sample size and by retrospective analysis. |

**Supplementary Table S3.** Correlation between HOXB9 expression and clinico-pathologic characteristic in bevacizumab treated colorectal cancer patients

| **Characteristic** | **HOXB9 negative n = 14 (24.14%)** | **HOXB9 positive n = 44 (72.86%)** | ***P*** |
|---|---|---|---|
| **Age** | | | 0.55 |
| <69 years | 7 | 26 | |
| >69 years | 7 | 18 | |
| **Primary tumor size (T)** | | | 0.584 |
| T1-2 | 2 | 9 | |
| T3-4 | 12 | 34 | |
| **PS ECOG** | | | 0.453 |
| PS 0 | 10 | 29 | |
| PS 1-2 | 3 | 15 | |
| **Time of metastasis occurrence** | | | 0.663 |
| Metachronous | 6 | 16 | |
| Synchronous | 8 | 28 | |
| **Mutational status** | | | 0.187 |
| B-RAF/N-RAS Wild-type | 14 | 39 | |
| B-RAF/N-RAS Mutated | 0 | 5 | |
| **Liver metastasis** | | | 0.061 |
| No | 8 | 13 | |
| Yes | 6 | 31 | |
| **KRAS status** | | | 0.702 |
| Wild-type | 4 | 15 | |
| Mutated | 10 | 29 | |